

NIObIUM IMPURITy-DOPING STUDIES AT CORNELL AND CM COOL-DOWN DYNAMIC EFFECT ON Q_0 *

M. Liepe,[†] B. Clasby, R. Eichhorn, F. Furuta, G.M. Ge, D. Gonnella, T. Gruber, D.L. Hall, G. Hoffstaetter, J. Kaufman, P. Koufalas, J.T. Maniscalco, T. O'Connell, P. Quigley, D. Sabol, J. Sears, E.N. Smith, V. Veshcherevich,
CLASSE, Cornell University, Ithaca, NY 14853, USA

Abstract

As part of a multi-laboratory research initiative on high Q_0 niobium cavities for LCLS-II and other future CW SRF accelerators, Cornell has conducted an extensive research program during the last two years on impurity-doping of niobium cavities and related material characterization. Here we give an overview of these activities, and present results from single-cell studies, from vertical performance testing of nitrogen-doped nine-cell cavities, and from cryomodule testing of nitrogen-doped nine-cell cavities. We show that 2K quality factors at 16 MV/m well above the nominal LCLS-II specification of 2.7×10^{10} can be reached reliably by nitrogen doping of the RF penetration layer. We demonstrate that the nitrogen furnace pressure is not a critical parameter in the doping process. We show that higher nitrogen doping levels generally result in reduced quench fields, with substantial variations in the quench field between cavities treated similarly. We propose that this can be explained by the reduced lower critical field H_{c1} in N-doped cavities and the typical variation in the occurrence of defects on a cavity surface. We report on the results from five cryomodule tests of nitrogen-doped 9-cell cavities, and show that fast cool-down with helium mass flow rates above 2 g/s is reliable in expelling ambient magnetic fields, and that no significant change in performance occurs when a nitrogen-doped cavity is installed in a cryomodule with auxiliary components.

INTRODUCTION

Future CW operated large scale SRF linacs rely on the availability of very high efficiency SRF cavities, i.e. cavities with high intrinsic quality factors Q_0 at operating temperature (typically 1.8K to 2K) and operating accelerating fields (typically 15 to 20 MV/m). A prime example is LCLS-II, a CW SRF driven FEL to be constructed at SLAC, calling for nominal SRF nine-cell operating parameters of $E_{acc} = 16$ MV/m and Q_0 of 2.7×10^{10} at 2K. [1] For many years now Cornell has been working on high efficiency niobium SRF cavities, initially as part of developing the technology for the Cornell Energy-Recovery-Linac (ERL), resulting in a proof-of-principle operation of a seven-cell 1.3 GHz cavity in a test cryomodule with unprecedented high 2K Q_0 of 3.5×10^{10} . [2] Motivated partly by such promising results, and partly by the recent demonstration that high temperature diffusion of small amounts of foreign

atoms into the niobium rf surface can yield a dramatically reduced BCS surface resistance [3, 4], the LCLS-II project was adopted to employ high Q_0 SRF cavities. A collaborative effort between FNAL, JLab, and Cornell University was established in order to support the rapid development of procedures to minimize the LCLS-II cryogenic heat load by maximizing the Q_0 of nine-cell 1.3 GHz cavities for use in the LCLS-II linac. [5–7] The collaboration decided early on to focus on high temperature diffusion of nitrogen impurities into the niobium cavity wall as the technical route to increasing Q_0 in the LCLS-II cavities, a process discovered at FNAL to lower cryogenic loads by $\approx 50\%$. [3] The nitrogen doping process has the advantage of requiring only small changes to the standard cavity treatment process, but still needed to be fully developed and demonstrated on multi-cell cavities, including on cavities in cryomodule environments at the time the LCLS-II high Q_0 collaboration was formed. In this paper we give an updated overview of Cornell's contributions to this development process.

SINGLE-CELL N-DOPING STUDIES

As part of developing the nitrogen-doping protocol for the LCLS-II cavities, Cornell performed two dedicated studies on single-cell 1.3 GHz cavities. The goal was to explore optimal parameters, demonstrate robustness of the process in meeting specifications, study the impact of environmental factors and the cool-down process on cavity performance, and to improve understanding of the underlying processes resulting in reduced BCS resistance, but also reduced maximum fields. The cavity treatment parameters used in these two studies were as follows:

- A 20 min N-doping at 800°C, follow by 30 min anneal in vacuum at 800°C ("20N30" process), followed by different final vertical electropolishing (VEP) amounts. This process was applied to 5 single-cell cavities. The 2K performance results of the cavities in vertical test are shown in Fig. 1. [8] The average quench field of these 5 cavities is 27 MV/m, and the average Q_0 is 3.6×10^{10} at 2K and 16 MV/m.
- B 20 min N-doping at 900°C, follow by 30 min anneal in vacuum at 900°C, followed by alternating vertical electropolishing (VEP) and vertical performance testing. This heavy doping ("over-doing") process was applied to one single-cell cavity to study the impact of heavy N-doping, especially reducing the quench field. The

* Work supported, in part, by the US DOE and the LCLS-II Project and by NSF grant PHYS-1416318.

[†] MUL2@cornell.edu

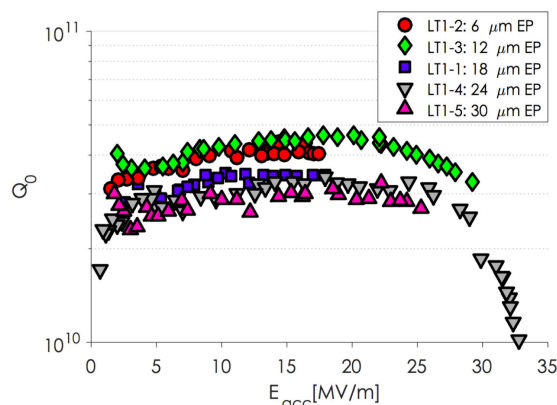


Figure 1: 2K Q_0 vs. E_{acc} performance of five N-doped 1.3 GHz single cell cavities using a 800°C "20N30" doping recipe with different final VEP amounts. [8]

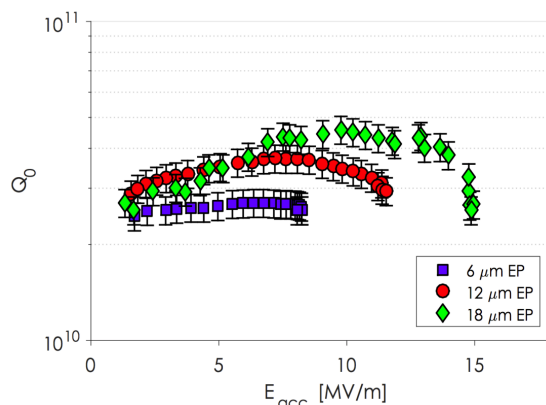


Figure 2: 2K Q_0 vs. E_{acc} performance of one N-doped 1.3 GHz single cell cavities using a 900°C "over-doping" recipe with different final VEP amounts. [9]

2K performance results of the cavities in vertical test are summarized in Fig. 2. [9]

The 800°C "20N30" process was found to reliably exceeded the LCLS-II specifications for a wide range of final VEP surface removal, relaxing tolerances on the optimal final removal amount, and allowing for additional surface chemistry if initial performance testing would indicate so. This process was therefore subsequently applied to nine-cell cavities as summarized in the next section. [8, 10] Higher doping levels (smaller final VEP amounts in the first study) resulted in generally higher 2K Q_0 values at 16 MV/m, with a substantial variation in maximum accelerating fields.

Figure 3 shows nitrogen pressure in the high temperature furnace during a typical 20 min N-doping run. There is a significant variation in the nitrogen pressure during the doping process due to nitrogen gas injection and nitrogen uptake by the cavity. Nevertheless, the nitrogen uptake by the niobium cavity (i.e. the nitrogen pressure drop in the furnace) follows a \sqrt{t} time dependence, as predicted by a simple diffusion model, and does not directly depend on the nitrogen pressure during the doping process. This demonstrates that the nitro-

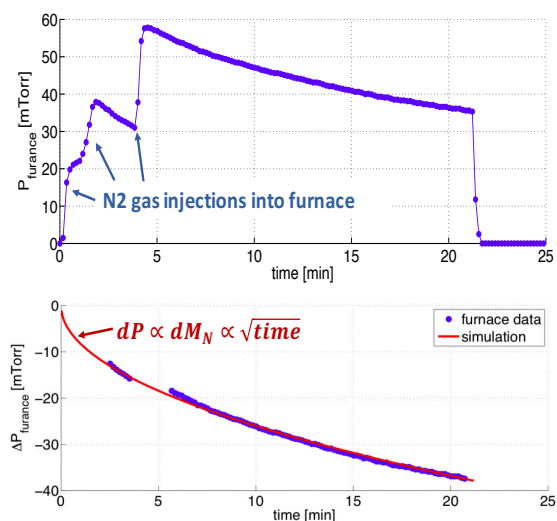


Figure 3: Top: Typical furnace nitrogen pressure during one of the 800°C "20N30" single-cell doping runs. Bottom: Predicted nitrogen pressure drop in the UHV furnace from a simple diffusion model compared with the measured pressure drop extracted from the graph shown above. The pressure drop follows the expected \sqrt{t} dependence, which shows that nitrogen uptake is not directly dependent on the nitrogen pressure. [9]

gen pressure is not a critical parameter in the doping process, making it a robust process depending only on temperature and time, which can be easily controlled.

Nitrogen-doped cavities show a greatly increased sensitivity to increased residual resistance due to trapped magnetic flux. [11, 12] Detailed studies on the cavities doped as part of the two studies discussed here showed that the lower mean free path (MFP) of the RF penetration layer of the N-doped cavities is responsible for this undesirable effect, but also demonstrated that this effect can be mitigated by very fast cool down with large spatial temperature gradients. Large spatial temperature gradients result in reduced trapping of ambient magnetic field, and therefore help minimize the increase in residual resistance by trapped flux. [13–15]

The N-doped single cell cavities showed a remarkable variation in quench field, with highest values similar to those of non-doped single-cell cavities, but low values well below typical quench fields of non-doped cavities. Figure 4 shows the maximum fields achieved in the N-doped single cell cavities for both the 800°C and 900°C recipes as function of the mean free path of the RF penetration layer and as function of the the final VEP amount. This data suggests that a minimum of several μm must be removed from the surface, especially after the 900°C doping, to achieve higher quench fields, likely because of the formation of NbN on the surface during the doping process [16]. The NbN formed during this process has very poor superconducting performance, and will go normal-conducting at modest fields, ultimately causing quench. It is further noteworthy that the doping process reduces the lower critical field H_{c1} by about 30% relative to

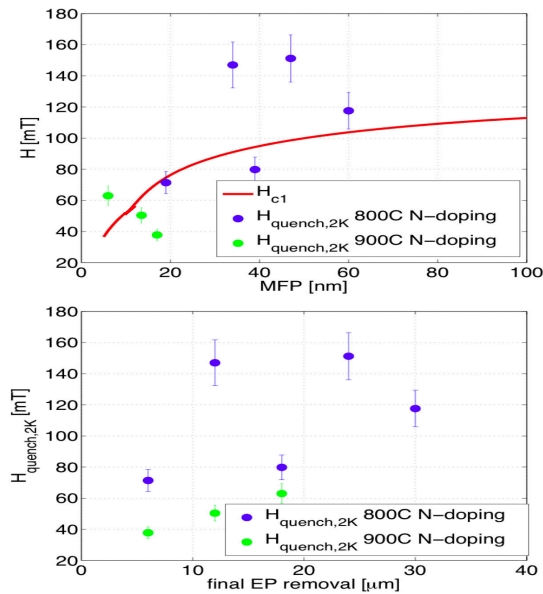


Figure 4: Top: Dependence of the lower critical field H_{c1} of niobium on mean free path (MFP) and measured quench fields of N-doped single-cell 1.3 GHz cavities vs. surface layer MFP extracted from surface impedance measurements. Bottom: Measured quench fields of N-doped single-cell 1.3 GHz cavities vs. final VEP amount after N-doping.

non-doped cavity grade niobium by reducing the mean free path (see Fig. 4), making N-doped cavities more susceptible to early flux entry at fields well below the ultimate limit set by the superheating field H_{sh} (which does only weakly decrease with reduced MFP) if defective areas are present on the cavity surface. Depending on the defects present on a cavity surface, N-doped cavities should then be expected to quench at maximum surface fields somewhere between H_{c1} and H_{sh} , as is indeed observed after sufficient final VEP to remove all NbN, as shown in Fig 4. Pulsed operation of a N-doped cavity confirmed that the quench field is in fact limited by a defect. [9]

The observed field dependency of the temperature dependent part of the surface resistance in nitrogen doped cavities can be well described by assuming a field dependent effective energy gap as shown in Fig. 5. [17] This is in agreement with recent theoretical work, suggesting that the density of states can have a significant dependence on surface fields. [18]

MULTICELL N-DOPED CAVITY PERFORMANCE

Five bare nine-cell 1.3 GHz cavities were nitrogen doped and vertically tested at Cornell. Figure 6 summarizes their measured 2K performances. The average quench field and average Q_0 exceed the nominal LCLS-II cavity performance specifications, demonstrating that the doping protocol originally developed on single-cell cavities was successfully transferred to multi-cell cavities. For details on the nine-cell cavity performances, refer to [10]. In the following we

Fundamental SRF R&D - Bulk Nb

C07-Processing Studies (doping, heat treatment)

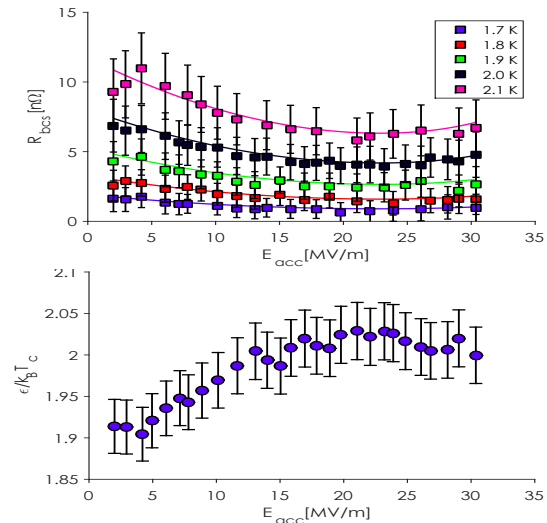


Figure 5: Top: Temperature dependent part of the measured surface resistance of a N-doped single-cell 1.3 GHz cavity vs. E_{acc} at different temperatures. Solid lines show calculated resistances based on BCS theory, assuming a field dependent effective energy gap as shown in the bottom graph, and using measured low field values for the remaining parameters (critical temperature, MFP). [17] Bottom: Effective field dependent energy gap vs. E_{acc} extracted from measured surface resistances shown in the top graph.

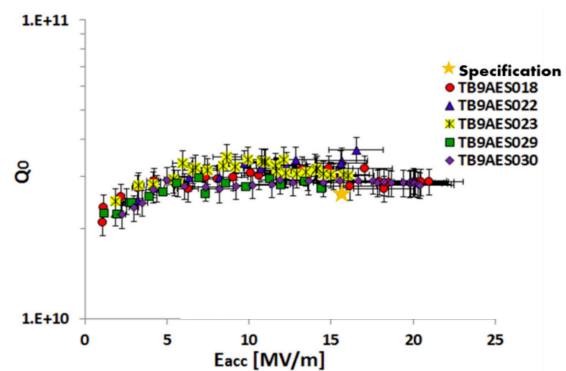


Figure 6: Best 2K Q_0 vs. E_{acc} performance of 5 bare nine-cell cavities N-doped and vertically tested at Cornell. Also shown is the LCLS-II nominal accelerating field and Q_0 specification. Cavities TB9AES018, TB9AES022, TB9AES023, and TB9AES029 received a 800°C "20N30" doping, while TB9AES029 was doped using a 800°C "6N6" recipe. Average quench field: 18 MV/m. Average Q_0 : 3.0×10^{10} . [10]

will restrict our discussion to the performances of two of the nine-cell cavities (TB9AES030 and TB9AES022), as these highlight important characteristics of quench fields in nitrogen doped cavities.

Cavity TB9AES030 was initially tested after N-doping using the "20N30" recipe, and subsequently retested after a surface reset and a "6N6" doping, resulting in a lower doping level. Figure 7 shows the 2K performances from these two

ISBN 978-3-95450-178-6

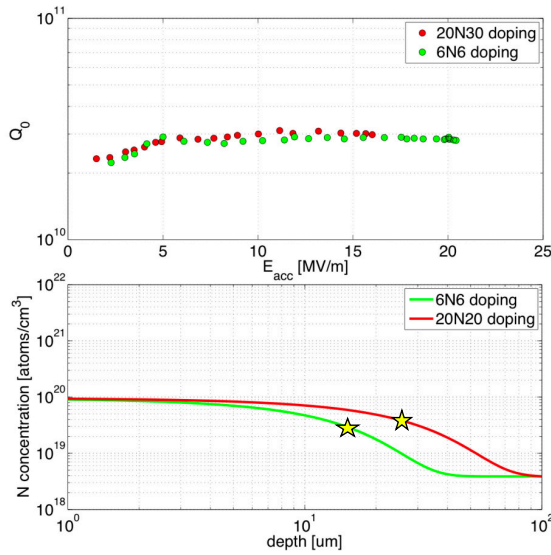


Figure 7: Top: 2K Q_0 vs. E_{acc} performance of nine-cell cavity TB9AES030 after initial "20N30" doping with 26 μm final VEP and after "6N6" doping with 14 μm final VEP following a 40 μm surface reset to remove the initial doping. Bottom: Simulated nitrogen concentration vs. depth into the material for the two 800°C doping recipes. The two stars make the simulated concentration levels at the surface after the corresponding final VEP.

tests in addition to simulated nitrogen concentration profiles for the two doping protocols. While the quality factors (and BCS surface resistances) are very similar for the two doping treatments, there is a clear increase in the quench field for the thinner and lower (after final VEP) concentration level "6N6" doping. This increase in maximum field can be attributed to either the higher H_{c1} due to the lower doping level, or to the thinner doping layer, which has very poor thermal conductivity due to its low RRR of the order of 10, or to a combination of both effects.

Cavity TB9AES030 was tested prior to doping to obtain a baseline performance, and then again after a short 800°C "2N2" N-doping. Figure 8 compares the 2K performances from these two tests, showing a $\approx 30\%$ reduction in quench field after the doping. Temperature mapping was used during both test to determine quench location, and it was found that in both cases, the cavity quench was triggered by exactly the same location in the high magnetic field region of one of the cells. Subsequent optical inspection of the quench location showed a large protuberance, which will cause significant magnetic field enhancement, and thus can cause quench. The observed 30% reduction in quench field corresponds well to the $\approx 30\%$ reduction in H_{c1} by the nitrogen doping, supporting the conclusion that the lower quench field in nitrogen doped cavities is indeed a consequence of earlier flux entry at defects in doped cavities due to a reduced lower critical field. This is further supported by the fact that nitrogen doped nine-cell cavities on average show a 30%

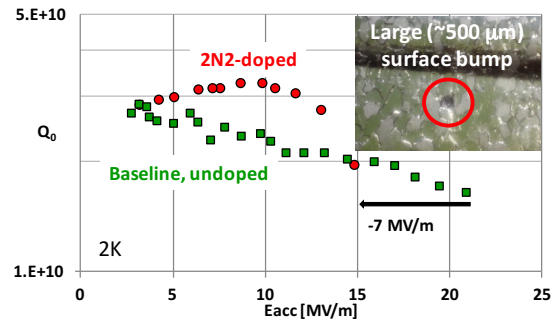


Figure 8: 2K Q_0 vs. E_{acc} performance of nine-cell cavity TB9AES022 before doping (baseline) and after 800°C "2N2" N-doping. In both tests, quench was caused by the same surface protuberance shown in the insert on the top right.

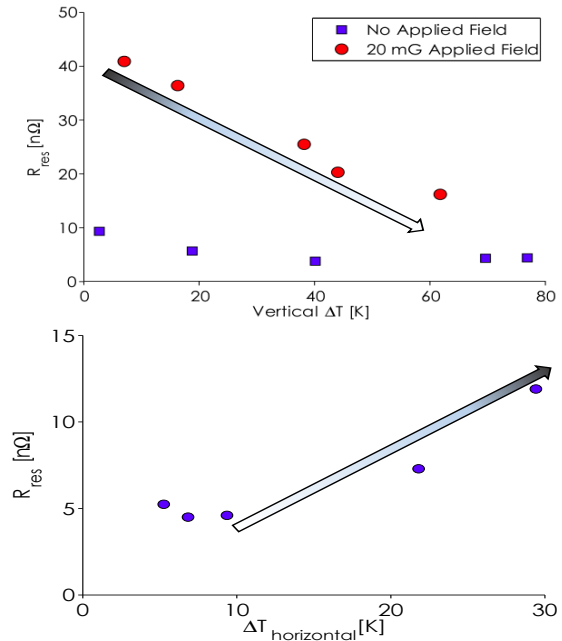


Figure 9: Top: Measured residual surface resistance of a "20N30" N-doped nine-cell cavity in the Cornell HTC vs. vertical temperature gradient over the cavity when starting to transition from the normal-conducting to the superconducting state. Shown are two cases: without applied DC magnetic field at the cavity location (< 5 mG ambient magnetic field) and with 20 mG applied DC magnetic field, produced by a solenoid wrapped around the outside of the cavity. [15] Bottom: Measured residual surface resistance of a "20N30" N-doped nine-cell cavity in the Cornell HTC vs. horizontal temperature gradient over the cavity when transitioning from the normal-conducting to the superconducting state.

to 40% (depending on doping level) lower average quench field [7] than the non-doped EXFEL cavities. [19]

Table 1: Comparison of the measured 2K Q_0 performance (at 16 MV/m or maximum field) of dressed N-doped 9-cell cavities in vertical (VT) performance test (tested at FNAL) and in the Cornell HTC, and corresponding change in surface resistance

| HTC test | Cavity ID | Q_0 in VT | Q_0 in HTC | $\Delta R_{VT \rightarrow HTC}$ [n Ω] |
|----------|-----------|--------------------------------|--------------------------------|---|
| HTC9-1 | TB9ACC012 | $(3.5 \pm 0.4) \times 10^{10}$ | $(3.2 \pm 0.3) \times 10^{10}$ | 1 ± 2 |
| HTC9-2 | TB9AES011 | $(3.4 \pm 0.3) \times 10^{10}$ | $(2.7 \pm 0.3) \times 10^{10}$ | 2 ± 2 |
| HTC9-3 | TB9AES018 | $(2.2 \pm 0.3) \times 10^{10}$ | $(2.2 \pm 0.2) \times 10^{10}$ | 0 ± 2 |

CRYOMODULE TESTING OF N-DOPED CAVITIES

The Cornell Horizontal-Test-Cryomodule (HTC) is a one-cavity cryomodule dedicated to testing high Q_0 SRF cavities in CW operation under realistic cryomodule conditions. [2] The cross-section of the HTC very closely resembles that of the planned LCLS-II cryomodules, and therefore allows performance testing of the nitrogen doped cavities under highly representative of conditions, i.e. operationally realistic cryogenic, vacuum, RF, and mechanical interfaces. Five tests of nitrogen doped cavities were performed in the HTC as part of the LCLS-II high Q_0 R&D program.

The first two HTC tests of nitrogen doped cavities not only were the first cryomodule tests of nitrogen doped cavities meeting LCLS-II specifications, but also highlighted important differences in the cool-down of cavities in the vertical and horizontal orientation, and in the importance of thermo-electric current induced magnetic fields. [20] Vertical temperature gradients over the cavity during fast cool-down are essential to minimize trapping of ambient magnetic fields and resulting increase in residual resistance, see Fig. 9 (top). Helium flow rates of >2 g/s were needed for efficient magnetic field expulsion by vertical temperature gradients. [15] However, horizontal temperature gradients during cool-down will generate thermo-electric currents, which can generate significant magnetic fields of tens of mG. In the horizontal cavity orientation, the vertical temperature gradients in addition to the horizontal gradients will then lead to a non-axial-symmetric current flow through the cavity, with magnetic fields at the RF penetration layer. Part of these fields will be trapped, even in fast cool-down, and result in increased residual resistance as is shown in Fig. 9 (bottom). Protocols and parameters for fast cavity cool-down in a cryomodule were developed, with large (10 to 30K) vertical temperature gradients for efficient and reliable expulsion of ambient magnetic field and small horizontal temperature gradients (< 10 K) to keep the impact of thermal-electric currents on R_{res} small. [15, 20–22]

The HTC tests of the nitrogen doped cavities showed no significant change in performance when the cavities were installed in the cryomodule, compared to the performance of the dressed cavities (cavity welded into a helium vessel) in vertical test dewars; see Fig. 10 and Table 1. No significant increase in the 2K cryogenic load or degradation in the cavity performance was observed after installation of the high power RF input coupler in the 4th HTC test. [15].

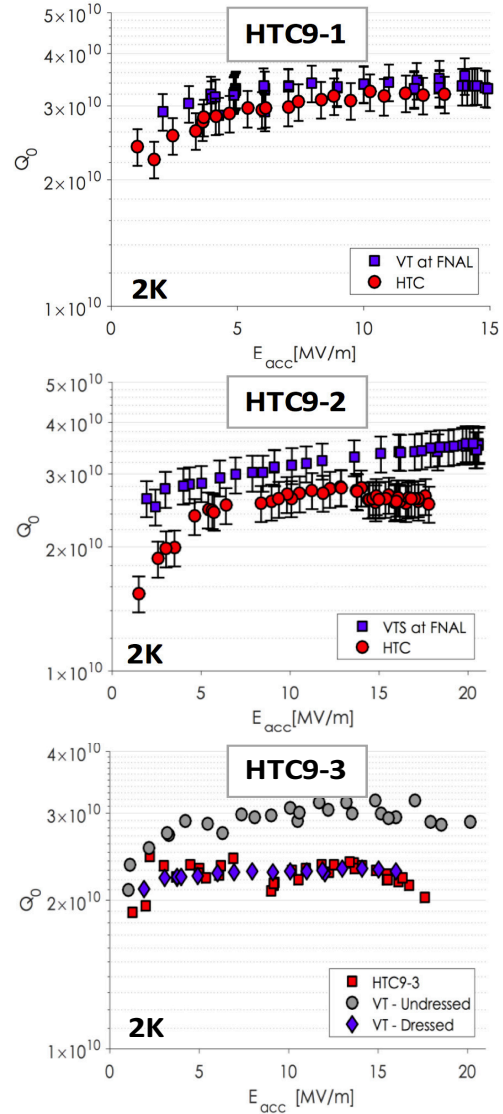


Figure 10: 2K Q_0 vs. E_{acc} performances of three dressed N-doped nine-cell cavities in vertical test at FNAL and in horizontal test in the Cornell HTC. [22]

A short (due to a cavity fabrication error) and multipacting in one of the HOM antennas during the 5th HTC test of a fully equipped nitrogen-doped cavity prevented reaching fields above 10 MV/m and caused significant heating, but still allowed for important frequency tuner, microphonics, and cavity frequency control studies. [23]

ACKNOWLEDGMENTS

The work presented here has been enabled by large numbers of technical and engineering staff at Cornell. Our thanks go to them all for their hard work and dedication. We also thank our colleagues at FNAL and TJNAF for a fruitful collaboration on developing the process for the high Q_0 cavities for LCLS-II, and for providing some of the N-doped cavities tested in the Cornell HTC.

REFERENCES

- [1] J. Galayda et al., in 27th Linear Accelerator Conference, Geneva, Switzerland, (2014), p. 404.
- [2] N. Valles, et al., "Record Quality Factor Performance of the Prototype Cornell ERL Main Linac Cavity in the Horizontal Test Cryomodule," in Proceedings of SRF13, Paris, France (2013).
- [3] A.Grassellino et al., "Nitrogen and argon doping of niobium for superconducting radio frequency cavities: a pathway to highly efficient accelerating structures," *Superconductor Science and Technology*, 26(102001), (2013).
- [4] P. Dhakal et al., "Effect of high temperature heat treatments on the quality factor of a large-grain superconducting radio-frequency niobium cavity," *Phys. Rev. ST Accel. Beams*, 16:042001, (2013).
- [5] A. Crawford, et al., "The Joint High Q0 R&D Program for LCLS-II," in International Particle Accelerator Conference 2014, Dresden, Germany, (2014), p. 2627.
- [6] C. Reece, "High-Q development plan and choice of Q0," LCLSII-4.5-EN-0216, SLAC, (2014).
- [7] P. Bishop, et al., "LCLS-II SRF Cavity Processing Protocol Development and Baseline Cavity Performance Demonstration," in 17th International Conference on RF Superconductivity, Whistler, Canada, (2015).
- [8] D. Gonnella, et al., in 27th Linear Accelerator Conference, Geneva, Switzerland, (2014), p. 866.
- [9] D. Gonnella, et al., "Fundamental Studies on Doped SRF Cavities," in 17th International Conference on RF Superconductivity, Whistler, Canada, (2015).
- [10] G.M. Ge, et al., "Performance of Nitrogen-Doped 9-Cell SRF Cavities in Vertical Tests at Cornell University," in 17th International Conference on RF Superconductivity, Whistler, Canada, (2015).
- [11] D. Gonnella and M. Liepe, "Flux Trapping in Nitrogen-Doped and 120 C Baked Cavities," Proceedings of IPAC14, Dresden, Germany (2014).
- [12] D. Gonnella, et al., "Sensitivity of Niobium Superconducting rf Cavities to Magnetic Field," in 17th International Conference on RF Superconductivity, Whistler, Canada, (2015).
- [13] A.Romanenko, et al., "Dependence of the residual surface resistance of SRF cavities on the cooling rate through T_c ," *J. Appl. Phys.*, 115(184903), (2014).
- [14] D. Gonnella, et al., in 27th Linear Accelerator Conference, Geneva, Switzerland, (2014), p. 84.
- [15] D. Gonnella, et al., in 6th International Particle Accelerator Conference, Richmond, VA (2015), p. 3446.
- [16] Y. Trenikhina, et al., "Nanostructure of the Penetration Depth in Nb Cavities: Debunking the Myths and New Findings," in 17th International Conference on RF Superconductivity, Whistler, Canada, (2015).
- [17] P.N. Koufalis, et al., in 17th International Conference on RF Superconductivity, Whistler, Canada, (2015).
- [18] A. Gurevich, "Reduction of dissipative nonlinear conductivity of superconductors by static and microwave magnetic fields," *Phys. Rev. Lett.*, 113(087001), (2014).
- [19] D. Reschke, "Recent Progress with EU-XFEL," in 17th International Conference on RF Superconductivity, Whistler, Canada, (2015).
- [20] D. Gonnella et al., "Nitrogen-doped 9-cell cavity performance in a test cryomodule for LCLS-II", *J. Appl. Phys.*, 117:023908, (2015).
- [21] D. Gonnella, et al., in 27th Linear Accelerator Conference, Geneva, Switzerland, (2014), p. 88.
- [22] D. Gonnella, et al., "Cryomodule Testing of Nitrogen-doped Cavities," in 17th International Conference on RF Superconductivity, Whistler, Canada, (2015).
- [23] W. Schappert, et al., "Resonance Control for Narrow Bandwidth SRF Cavities," in 17th International Conference on RF Superconductivity, Whistler, Canada, (2015).